



The Effects of Heat Generation/Absorption and Magnetic Field on Marangoni Flow of a Nanofluid Containing Gyrotactic Microorganisms Over a Stretching Surface

Elsayed MA Elbashbeshy*

Mathematics Department, Faculty of Science, Ain Shams University, Abbassia, Cairo, Egypt

Submission: March 07, 2023; **Published:** April 05, 2023

***Corresponding author:** Elsayed MA Elbashbeshy, Mathematics Department, Faculty of Science, Ain Shams University, Abbassia, Cairo, Egypt

Abstract

The current study examines the numerical approximation of Marangoni flow of a Nanofluid containing gyrotactic microorganisms over a stretching surface in the presence heat generation and magnetic field. The governing equations are written down and converted into a system of nonlinear ordinary differential equations. The resultant system is solved numerically. Discussion and analysis are conducted on the impacts of the factors on the velocity, temperature, concentration, and density of motile microbe. Additionally, computed and explored for various embedded factors in the issue statements are the density of the motile microbe, Nusselt number, Sherwood number, and skin friction coefficient.

Keywords: Marangoni Flow; Stretching Surface; Heat, And Mass Transfer; Gyrotactic Micro-Organism; Magnetic Field; Heat Generation

Introduction

The mass transfer across an interface between two fluids caused by a differential in surface tension is known as the Gibbs-Marangoni effect. This aspect is referred to as thermo-capillary convection or Bénard-Marangoni convection in the event of temperature dependency. In fact, Marangoni convection, which is brought on by changes in surface tension gradients (i.e., temperature and concentration gradients), finds significant use in the processing of silicon wafers, soap films, nucleation of vapor bubbles, spreading of thin films, and other semi-conductor-related fields. In their study of Marangoni-driven boundary layer flow in nanofluids, Nazar et al. [1] found that heat transmission is enhanced more effectively by nanoparticles with poor thermal conductivity. Marangoni convection has been studied by several scholars in a variety of geometries [2-5]. Arifin et al. [6] inspected the influence of radiation on Marangoni convection boundary layer flow of nanofluid and found that a raise in thermal radiation parameter reduces the quota of heat transmitted at the surface. Copper-water nanofluid flow and heat transport through a porous medium disc were studied by Yanhai and Liancun [7]. Ambrish et al. [8] study the mathematical Marangoni Convection MHD Flow of Carbon Nanotubes across a Porous Medium. The impact of MHD Marangoni Convective Flow of Nanofluid through a porous medium with heat and mass transfer was investigated by Venkateswara

Raju et al. [9]. The habitation of heavy microbe collecting on top of lighter water is what causes the phenomena of bio-convection in nanofluid, which is the subject of current investigation. The establishment of the bio-convection process within the system happens when the heavier bacteria fall into the water and are replaced by up floating microbe. A macroscopic motion is caused by the mesoscale phenomena of moving motile Microbe (convection). The literature: [10-21] covers the evolution of theoretical work in bio-convection. The properties of heat transport in the laminar boundary layer of a viscous fluid over a stretched sheet with viscous dissipation or frictional heating and internal heat generation were examined by Vajravelu and Haidilao [22]. Vajravelu and Hadjinolaou [22] estimated the volumetric rate of heat production in their investigation to be

$$q^* = \begin{cases} Q_0(T - T_\infty) & \text{for } T \geq T_\infty \\ & \text{for } T \leq T_\infty \end{cases}$$

Where Q_0 is the heat generation/absorption constant. The relationship mentioned above, as Vajravelu and Hadjinolaou [22] stated, is accurate as a state approximation for various exothermic processes using T_∞ as the onset temperature. They employed

$q^{*} = Q_0(T - T_{\infty})$ when the input temperature was not less than T_{∞} . It is clear from the research reviewed above that the issue of Marangoni flow, heat, mass, and motile microbe transmission over a stretching surface has not yet been taken into consideration.

Mathematical Model

As exhibited in Figure 1, the current study takes the effects of heat production into account as a constant two-dimensional incompressible Marangoni convective boundary layer flow of a nanofluid across a stretched surface. The coordinates are x

and y along the stretching surface and normal to it, respectively. Suppose that flow occurs across $y \geq 0$. A uniform transverse magnetic field of strength B_0 is implemented in y -direction, The magnetic Reynolds number is taken to be small enough so that the induced magnetic field can be neglected. Also assume that $T(x)$, $C(x)$ and $N(x)$ represent the fluid’s temperature, concentration, and motile microbe density, respectively. Let’s assume that T_{∞} , C_{∞} , and N_{∞} are the corresponding amounts in the free stream. The surface tension depends on temperature, concentration, and density of motile Microbe such that

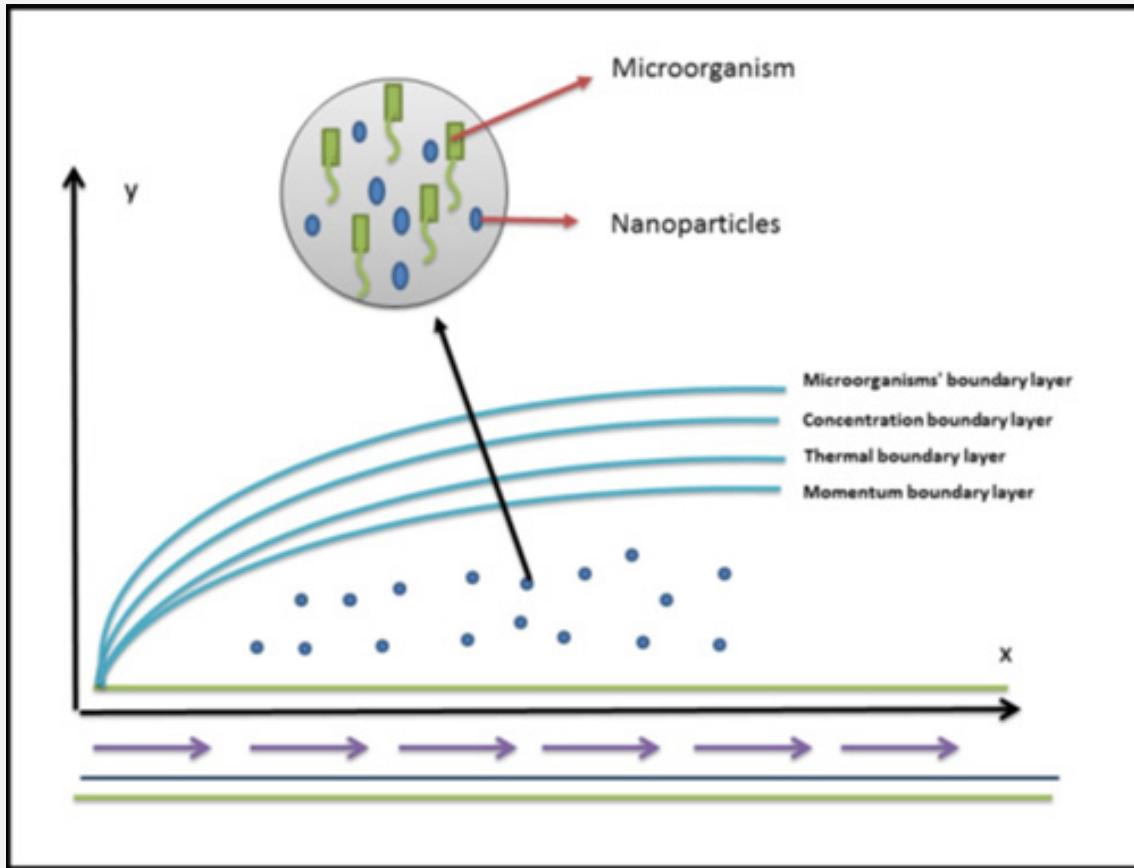


Figure 1: Schematic of flow above stretching surface.

$$\sigma = \sigma_0[1 - \gamma(T - T_{\infty}) - \gamma^*(C - C_{\infty}) - \gamma^{**}(N - N_{\infty})]$$

Where σ_0 is interface surface tension ratio and

$$\gamma = -\frac{1}{\sigma_0} \left(\frac{\partial \sigma}{\partial T} \right)_{C,N}, \quad \gamma^* = -\frac{1}{\sigma_0} \left(\frac{\partial \sigma}{\partial C} \right)_{T,N}, \quad \gamma^{**} = -\frac{1}{\sigma_0} \left(\frac{\partial \sigma}{\partial N} \right)_{T,C}$$

The following are the governing equations for this investigation: (Figure 1).

$$\frac{\partial u}{\partial x} + \frac{\partial v}{\partial y} = 0, \tag{1}$$

$$\left(u \frac{\partial u}{\partial x} + v \frac{\partial u}{\partial y} \right) = \nu \left(\frac{\partial^2 u}{\partial y^2} \right) - \frac{\sigma^* B_0^2}{\rho_{\infty}} u, \tag{2}$$

$$u \frac{\partial T}{\partial x} + v \frac{\partial T}{\partial y} = \alpha \left(\frac{\partial^2 T}{\partial y^2} \right) + \tau \left[D_B \left(\frac{\partial T}{\partial y} \frac{\partial C}{\partial y} \right) + \frac{D_T}{T_{\infty}} \left(\frac{\partial T}{\partial y} \right)^2 \right] + Q_0(T - T_{\infty}) \tag{3}$$

$$u \frac{\partial C}{\partial x} + v \frac{\partial C}{\partial y} = D_B \left(\frac{\partial^2 C}{\partial y^2} \right) + \frac{D_T}{T_{\infty}} \left(\frac{\partial^2 T}{\partial y^2} \right), \tag{4}$$

$$\frac{\partial N}{\partial x} + v \frac{\partial N}{\partial y} = D_n \left(\frac{\partial^2 N}{\partial y^2} \right) - \frac{bW_c}{C_w - C_\infty} \left[\frac{\partial}{\partial y} N \left(\frac{\partial C}{\partial y} \right) \right], \quad (5)$$

with boundary conditions

$$\text{at } y = 0: \mu \frac{\partial u}{\partial y} = \frac{\partial \sigma}{\partial x}, \quad v = 0, \quad T = T_w, \quad C = C_w, \quad N = N_w$$

$$\text{as } y \rightarrow \infty: u \rightarrow 0, \quad T \rightarrow T_\infty, \quad C \rightarrow C_\infty, \quad N \rightarrow N_\infty \quad (6)$$

where ν is the kinematic viscosity, where σ^* is the electrical conductivity, ρ_∞ is the density of fluid, τ the ratio of the effective heat capacitance of the nanoparticle to that of the base fluid, α is the thermal diffusivity of the fluid, T_w is the surface temperature, C_w is the surface concentration, N_w is the surface density of microorganism, D_B , D_T and D_n are the Brownian diffusion coefficient, thermophoresis diffusion coefficient and diffusivity of micro-organisms, respectively, b is the chemotaxis constant, W_c is maximum cell swimming speed, bW_c is assumed to be constant, and Q_0 is the heat generation or absorption coefficient such that $Q_0 > 0$ corresponds to heat generation while $Q_0 < 0$ corresponds to heat absorption.

Select a stream function $\psi(x, y)$ such that the equation of continuity is fulfilled. So

$$u = \frac{\partial \psi}{\partial y}, \quad v = -\frac{\partial \psi}{\partial x}.$$

Introducing the following similarity variables:

$$\theta(\gamma, z) = \nu X f(\xi), \quad \xi = \frac{y}{L}, \quad X = \frac{x}{L}, \quad \xi(\xi) = \frac{T - T_\infty}{T_w - T_\infty}, \quad T_w - T_\infty = T_0 X^2,$$

$$\phi = \frac{C - C_\infty}{C_w - C_\infty}, \quad C_w - C_\infty = C_0 X^2, \quad X = \frac{N - N_\infty}{N_w - N_\infty}, \quad N_w - N_\infty = N_0 X^2,$$

Where T_0 is the reference temperature, C_0 is the reference concentration and N_0 is the reference density of micro-organisms. Equations (2), (3), (4) and (5) can be written as

$$f''' - f'^2 + ff'' - \xi f' = 0, \quad (7)$$

$$\theta'' + \text{Pr} f \theta' - 2 \text{Pr} f' \theta + \text{Pr} N_b \phi \theta' + \text{Pr} N_t \theta'^2 + \lambda \text{Pr} \theta = 0, \quad (8)$$

$$\phi'' = \text{Sc} f \phi' + \frac{N_t}{N_b} \theta'' = 0, \quad (9)$$

$$X'' + \text{Le} f X' - 2 \text{Le} f' X - \text{Pe} [(x + \delta) \phi'' + \phi' X'] = 0, \quad (10)$$

with boundary conditions

$$\eta = 0: f = 0, \quad f''(0) = -2(1 + \delta^*), \quad \theta = 1, \quad \phi = 1, \quad X = 1$$

$$\eta \rightarrow 0: f' = 0, \quad \theta = 0, \quad \phi = 0, \quad X = 0 \quad (11)$$

$$\xi = \frac{L^2 \sigma^* B_0^2}{\rho_\infty}$$

where ρ_∞ is the magnetic field parameter, $\text{Pr} = \frac{\nu}{\alpha}$ is the Prandtl number, $N_b = \tau D_B (C_w - C_\infty) / \nu$ is the Brownian motion parameter, $N_t = \tau D_T (T_w - T_\infty) / \nu T_\infty$ is the thermophoresis parameter, $\lambda = Q_0 L^2 / \alpha$ is the heat-source/sink parameter, $\text{Sc} = \nu / D_B$ is the Schmidt number, $\text{Le} = \nu / D_n$ is the Lewis number, $\text{Pe} = bW_c / D_n$ is the Peclet number, $\delta = N_\infty / (N_w - N_\infty)$ is motile Microbe parameter, L is a reference length and is defined as $L = \mu \nu / \gamma \sigma_0 T_0$ and δ^* can be introduced as $\delta^* = (\gamma^* c_0 + \gamma^{**} N_0) / \gamma T_0$.

physical quantities of practical significance in this work are the local Nusselt number Nu , and local Sherwood number Sh , and the local density number of the motile micro-organisms N_n which are expressed as

$$Nu = -\frac{x \left(\frac{\partial T}{\partial y} \right)_{y=0}}{(T_w - T_\infty)}, \quad Sh = -\frac{x \left(\frac{\partial C}{\partial y} \right)_{y=0}}{(C_w - C_\infty)}, \quad N_n = -\frac{x \left(\frac{\partial N}{\partial y} \right)_{y=0}}{(N_w - N_\infty)},$$

$$C_f = x R_e^{-2} f''(0), \quad Nu = -\frac{x}{L} \theta'(0), \quad Sh = -\frac{x}{L} \phi'(0), \quad N_n = -\frac{x}{L} X'(0)$$

Where U_w is the uniform stretching velocity of the surface.

Results and Discussion

In this segment, governing coupled ODEs [7-10] with suitable boundary conditions [11] have been solved numerically by utilizing the Runge-Kutta-Fehlberg method with the help of computational software MATHEMATICA.

Table 1 recognizes the fluctuations of the amended Nusselt number, $-\theta''(0)$, the amended Sherwood number, $-\phi''(0)$ and the amended density number of the motile Microbe $-X''(0)$. The effects of the magnetic parameter ξ on the fluid velocity boundary layers have tendency to produce a Lorentz force which acts in the direction opposite so that of the flow, causing a flow retardation effect. This causes the fluid velocity to decrease, as seen in Figure 2(a). On the other hand, enhancing the values of ξ grows the widths of the thermal, the concentration and density of motile microorganism profiles, as seen in Figures 2(b), 2(c) and 2(d). The relationship between a fluid's viscosity and thermal conductivity is known as the Prandtl number, which has no dimensions. As a result, it evaluates the relationship between a fluid's velocity and

its ability to transmit heat. Recognized that a larger Prandtl number fluid has a drop in heat conduction. For larger value of Pr , the fluid thermal boundary layer will be thinner, as shown in Figure 3(a). As depicted from Figure 3(b), the fluid concentration is

increased by increasing the value of Pr close to the surface, but the reverse situation is settled apart from the surface. As the fluid thermal boundary layer behaved, the density of motile microorganism profile behaves as shown in Figure 3(c).

Table 1: Fluctuations of amended Nusselt/Sherwood numbers.

ξ	Pr	Nb	Sc	λ	Sc	Le	Pe	δ	δ^*	$-\theta'(0)$	$-\phi'(0)$	$-x'(0)$
0.1	0.71	0.5	0.5	0.1	0.5	3	0.5	0.5	2	1.645715	0.453097	9.746505
0.5										1.589738	0.411041	9.513847
0.9										1.535616	0.372671	9.294786
0.3	0.71	0.5	0.1	0.1	0.5	1	0.5	0.5	2	1.61749	0.431624	5.422875
	1									1.932846	0.187554	5.348174
	2									2.628735	-0.37477	5.180795
0.3	0.71	0.5	0.5	0.5	0.5	0.5	0.5	0.5	2	1.499851	0.211612	3.745131
		1								1.356942	1.072332	3.883243
		1.5								1.230011	1.25438	3.927358
0.3	0.71	0.5	0	0.5	0.5	0.5	0.5	0.5	2	1.582078	1.517237	3.993665
			0.2							1.547979	1.100573	3.89299
			0.5							1.499851	0.511612	3.745131
0.3	0.71	0.5	0.5	-0.5	0.5	3	0.5	0.5	2	1.75603	0.330439	9.584359
				0						1.642617	0.413727	9.620554
				0.5						1.499851	0.511612	9.664395
0.3	0.71	0.5	0.5	0.5	0.5	0.5	0.5	0.5	2	1.499851	0.511612	3.745131
					0.7					1.465512	0.993882	3.867973
					1					1.429505	1.582873	4.004337
0.3	0.71	0.5	0.5	0.5	0.5	0.1	0.5	0.5	2	1.499851	0.511612	1.43486
						0.5				1.499851	0.511612	3.745131
						1				1.499851	0.511612	5.450837
0.3	0.71	0.5	0.5	0.5	0.5	0.5	0.1	0.5	2	1.499851	0.511612	1.697351
							0.5			1.499851	0.511612	1.935772
							1			1.499851	0.511612	3.745131
0.3	0.71	0.5	0.5	0.5	0.5	0.5	0.5	0.1	2	1.499851	0.511612	2.609682
								0.3		1.499851	0.511612	3.051287
								0.5		1.499851	0.511612	3.745131
0.3	0.71	0.5	0.5	0.5	0.5	0.5	0.5	0.5	0.5	1.070815	0.472774	2.957496
									1	1.245194	0.481294	3.261206
									1.5	1.383445	0.495637	3.519114

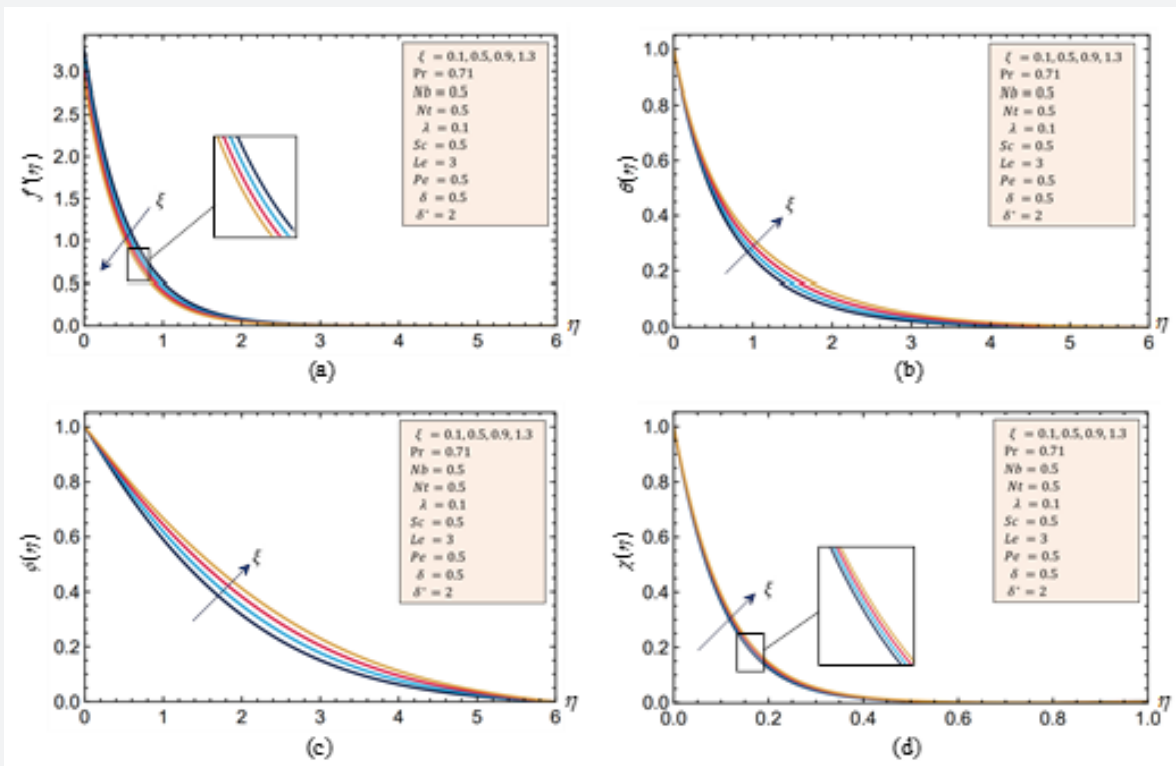


Figure 2: Velocity, temperature, concentration, and motile microorganism density charts influenced by ξ .

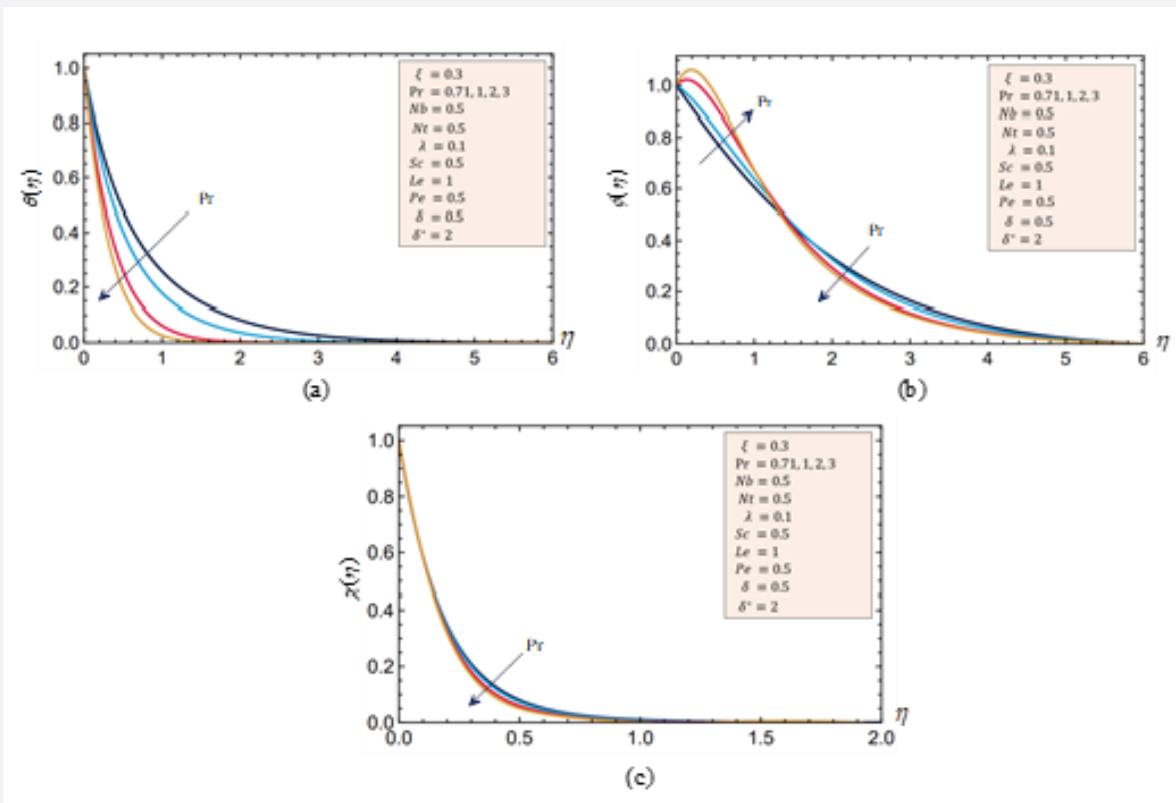


Figure 3: Temperature, concentration, motile microorganism density charts influenced by Pr .

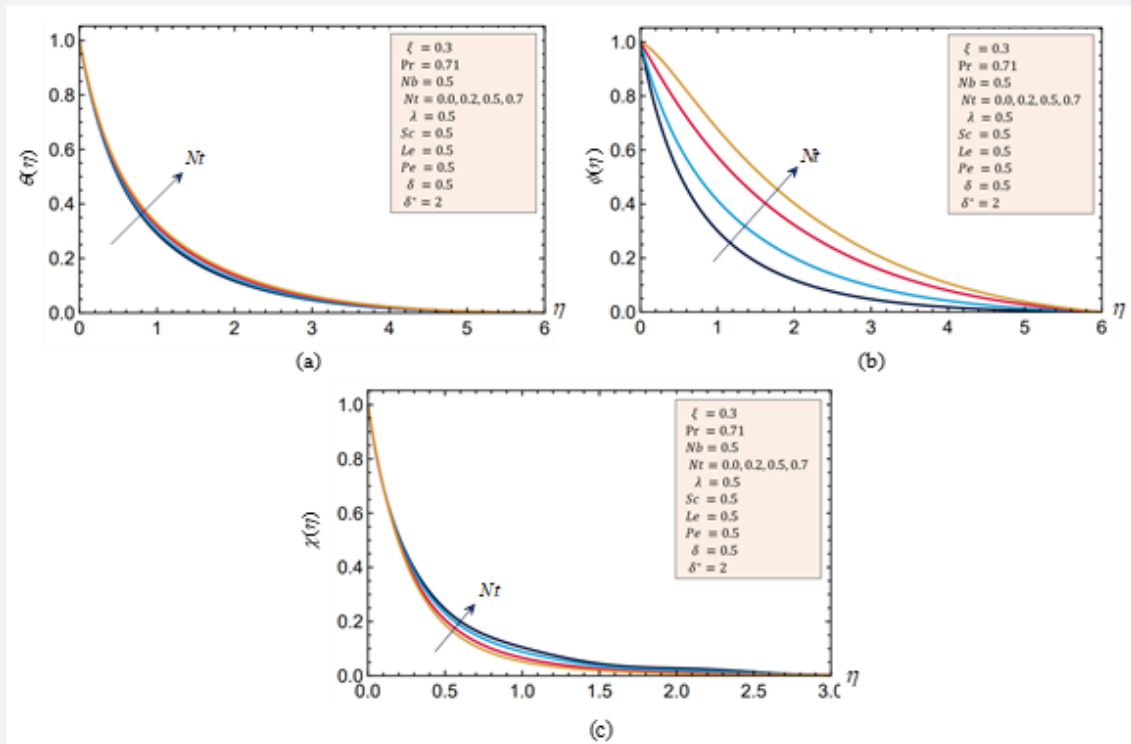


Figure 4: Temperature, concentration, motile microorganism density charts influenced by Nr .

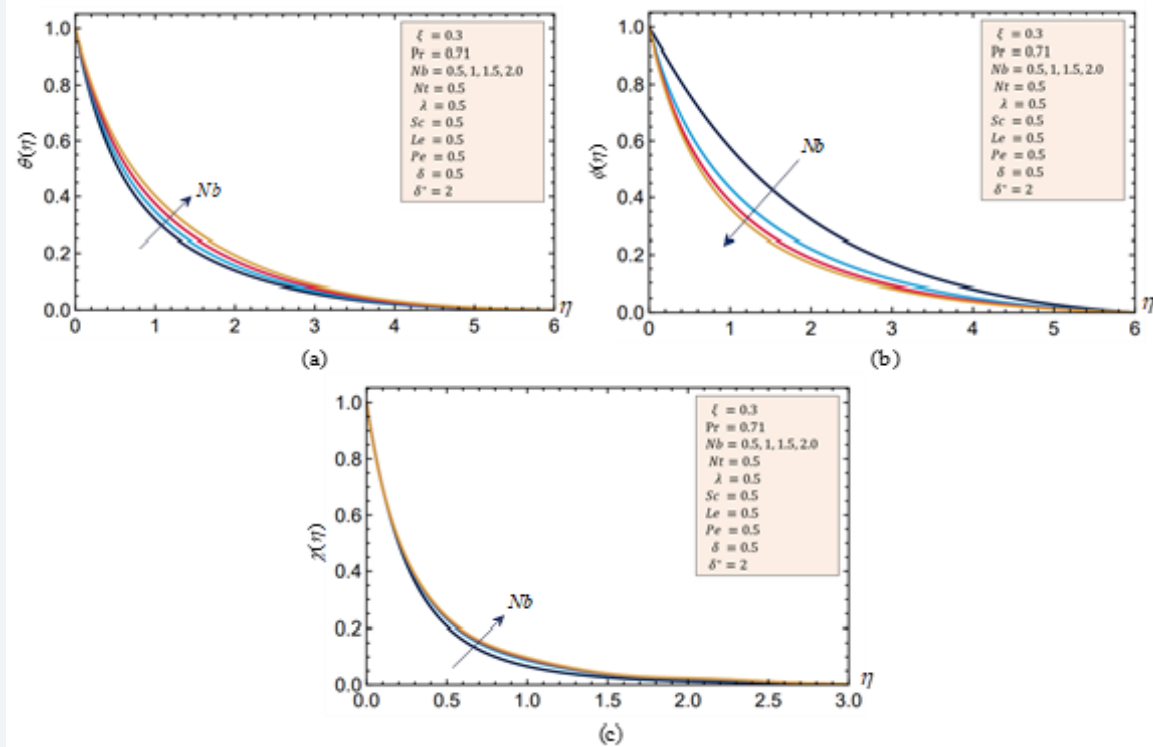


Figure 5: Temperature, concentration, motile microorganism density charts influenced by Nb .

Thermophoresis is a mechanism where various types of mobile particle mixes respond differently to the force of a temperature gradient. This study uses the thermophoresis parameter Nt to explain this occurrence. It's important to note that the thermophoresis parameter can have a positive or negative value, with the negative value of Nt denoting a hot surface and the positive value denoting a cool surface. A hot surface repels particles and motile microbes, as seen in Figures 4(b) and Figures 4(c), therefore thermophoresis tends to blast them away from the surface for hot surfaces. As a result, layer that is largely devoid of nanoparticles and mobile microbes develops just below the surface. As can be seen from Figure 4(a), raising Nt raises the temperature of the nanofluid. These findings can be explained by the fact that the nanofluid with the lower thermophoresis diffusion parameter has a greater volumetric heat capacity. As a result, the surface cools down and more heat is transmitted from the surface to the nanofluid. The random movement of nanoparticles floating in a fluid

known as Brownian diffusion is the result of their bombardment by the fluid's quickly moving atoms or molecules. The temperature and particle concentration in the boundary layer above the surface are controlled by this motion. The key to understanding Brownian motion is the Brownian motion parameter Nb . As can be seen from Figure 5(a), increasing Nb raises the temperature of the nanofluid. The nanofluid with the lowest Brownian diffusion parameter and the maximum volumetric heat capacity is one way to interpret these data. As a result, the surface cools down and more heat is transmitted from the surface to the nanofluid. On the other hand, as can be observed from Figure 5(b), increasing Nb causes the nanofluid concentration to drop. This effect is explained by the fact that an increase in Brownian diffusion would cause the nanoparticles to scatter more randomly away from the nanofluid's (higher concentration zone) surface (lower concentration zone). The density of the motile Microbe is slightly increased by increasing Nb as seen from Figure 5(c), (Table 1).

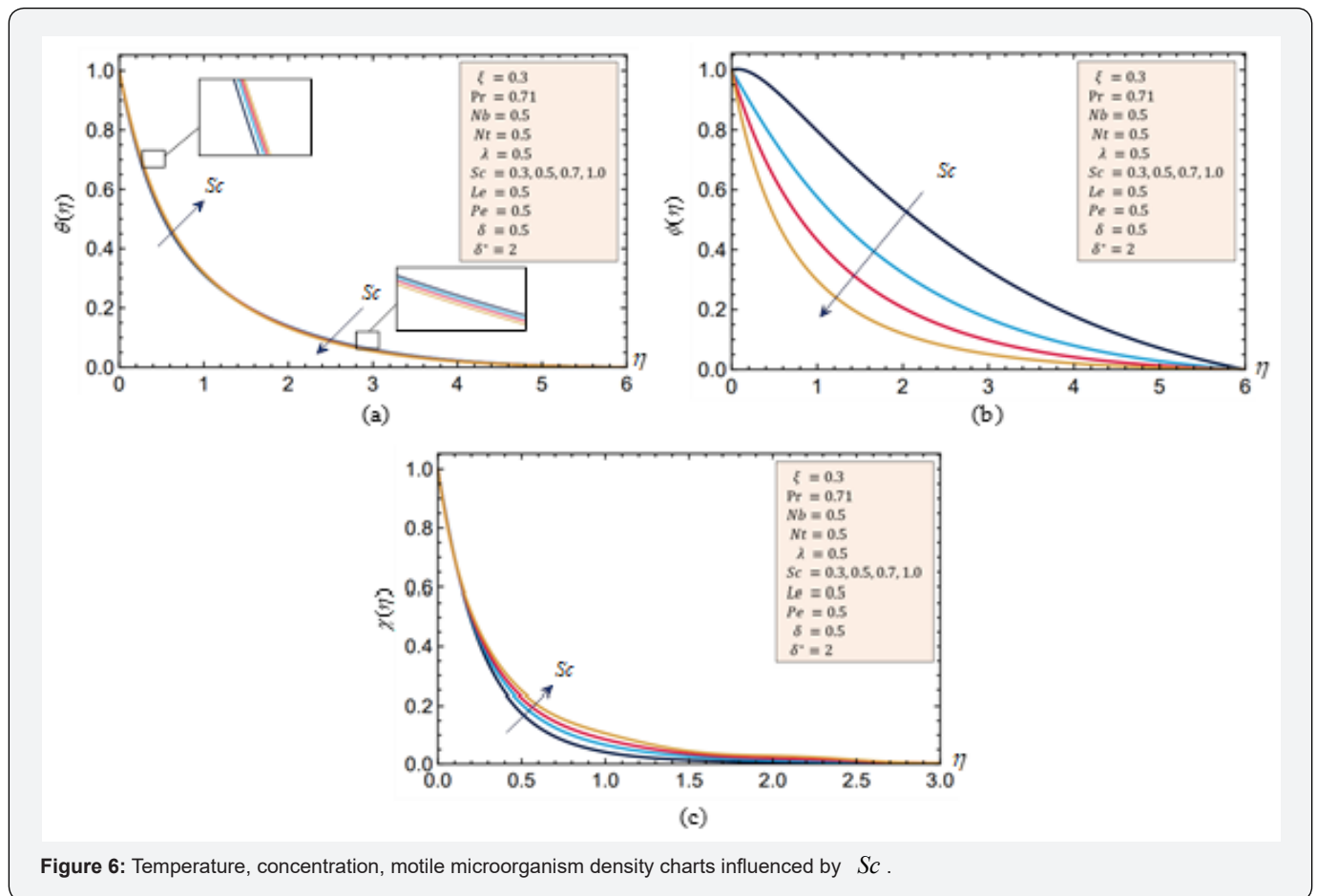


Figure 6: Temperature, concentration, motile microorganism density charts influenced by Sc .

Figure 6(c) depicts the effect of Schmidt number Sc on the density of motile Microbe. Close to the surface, the nanofluid temperature is increased slightly by increasing Sc while the reverse happens apart from the surface as exhibited in Figure 6(a). For bigger values of Sc , there is a downward tendency of concentration as seen from Figure 6(b). Physically, the concentration and

accompanying layers are reduced due to a decrease in mass diffusivity for bigger Sc . Heat generation/absorption, λ , is a non-dimensional metric that is dependent on the quantity of heat created or absorbed in the fluid. The fluid temperature is increased as figured out from Figure 7(a) which is anticipated whereas the heat generating engine enhances heat transferred from surface to

fluid and reverse takes place in case of heat absorption. Close to the surface, the nanofluid concentration is decreased slightly by increasing λ while the reverse happens apart from the surface as exhibited in Figure 7(b). The ratio of heat diffusivity to microorganism diffusivity is known as the bio-convection Lewis number. It is used to depict fluid flows where simultaneous microorganism and heat transfer is occurring. Figure 8(a) shows how the bio-convection Lewis number affects the motile microorganism profile.

In the boundary layer regime, bio-convection Lewis number is a measure of how much thermal diffusion rate contributes to microorganism diffusion rate. As a result, when $Le=1$, both heat and microorganism diffuse at the same rate, and when $Le>1$, heat diffuses more quickly than microorganism. As the bio-convection Lewis number rises, the motile microorganism boundary layer becomes thinner (Figure 2).

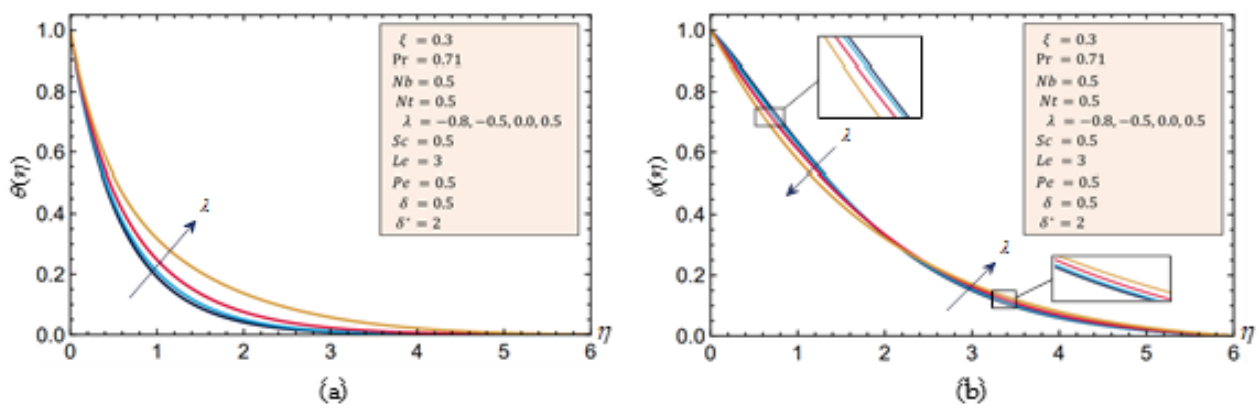


Figure 7: Temperature/concentration charts influenced by λ .

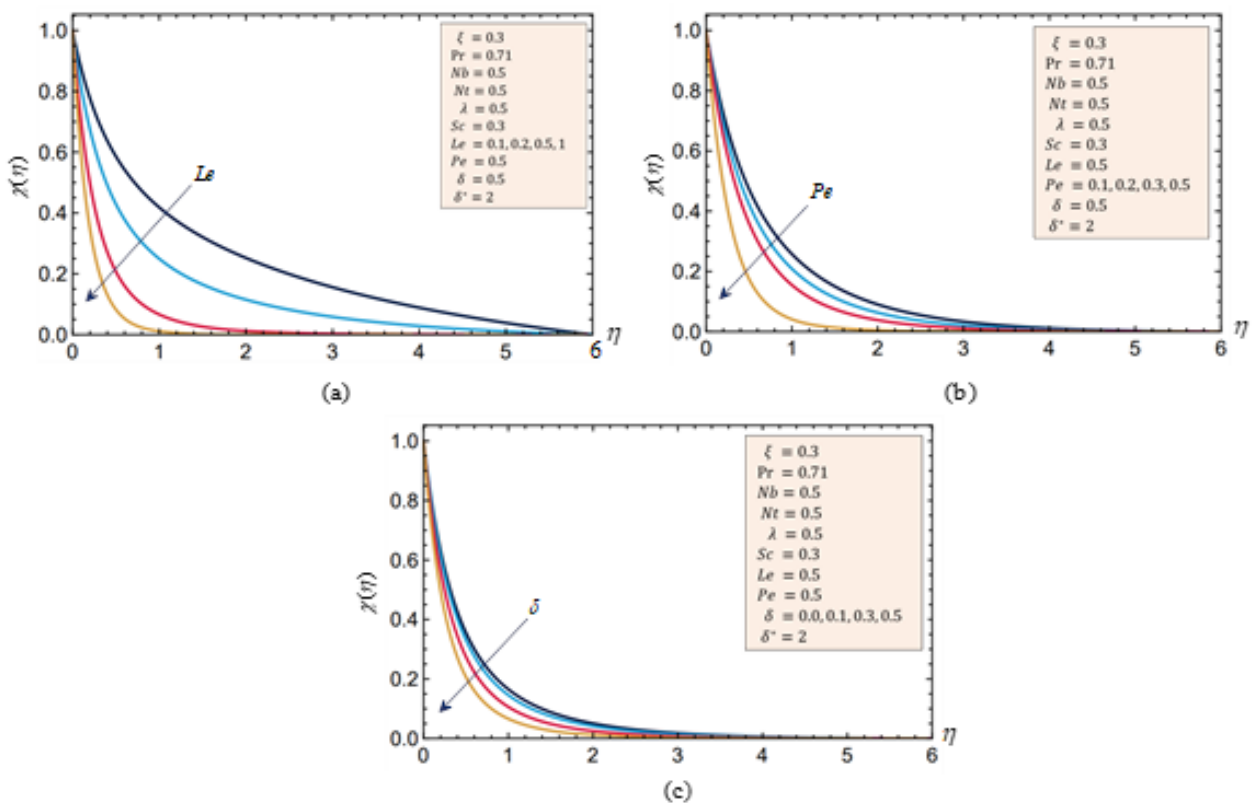


Figure 8: Motile microorganism density charts influenced by Le , Pe and δ , respectively.

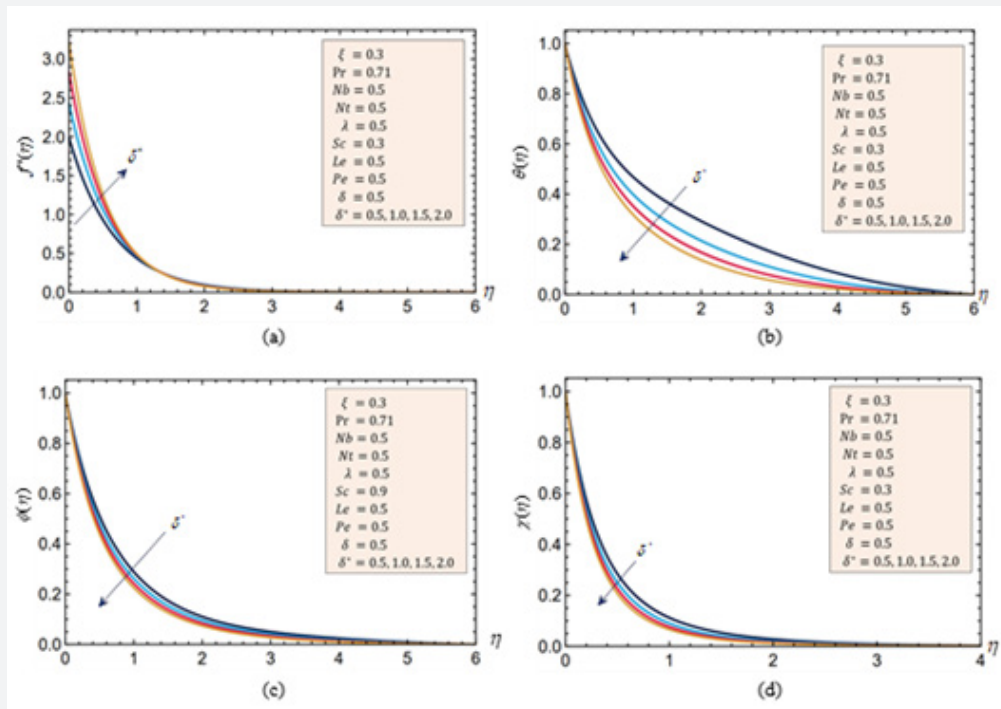


Figure 9: Velocity, temperature, concentration, and motile microorganism density charts influenced by δ^* .

A big bio-convection Peclet number suggests an advectively dominated distribution while a small number shows a diffuse flow. The bio-convection Peclet number measures the relative significance of advection vs diffusion. As a result, if the bio-convection Peclet number rises, the motile microorganism boundary layer becomes thinner as shown in Figure 8(b). An increase of motile Microbe parameter δ reduces the motile microorganism boundary layer as shown in Figure 8(c) (Figure 3-6). Examining the impact of surface tension on motion in light of the Marangoni convection effect is one of the main objectives of this study. With both heat and mass transmission, the physical values of γ and γ^* represent the gradient of the surface tension. When a result, as the surface tension parameter, δ^* , increases, the surface tension decreases (according to the negative values of the coefficients γ and γ^*). As a result, lowering the surface tension at the free surface lowers the free surface stiffness and enhances the free surface's capacity to move. As a result, as illustrated in Figure 9(a), the velocity increases (Figure 7,8). In addition, Figures 9(b), 9(c) and 9(d) show the impact of surface tension coefficients on heat, concentration, and motile Microbe, respectively. The conditions $T < T_\infty$, $C < C_\infty$ and $N < N_\infty$ are considered to be present throughout the boundary layer. In terms of physics, raising both the gradients of temperature, concentration and motile-microorganism density causes more instability at the contact by lowering the surface tension. As illustrated, raising the surface tension parameter lowers the temperature's, the concentrations, and the density of motile-microorganism's profiles.

Conclusion

The purpose of current investigation is to explore the impacts of heat production on Marangoni flow of a nanofluid containing gyrotactic Microbe across a stretched surface in the presence of magnetic field. Using an appropriate similarity transformation, the controlling boundary layer equations are written down and converted into ordinary differential equations. The numerically solve the resultant ordinary differential equations. Discussion and analysis are conducted on the impacts of the various factors on the velocity, temperature, concentration, and motile microbe density. Additionally, computed and explored for various embedded factors in the issue statements are the density of the motile microbe, the Nusselt number, Sherwood number, and the skin friction coefficient. The findings are visually displayed. It has been discovered that: The fluid velocity is reduced by enhancing magnetic parameter characteristic while it is increased by improving the surface tension. The fluid temperature is enhanced by enhancing permeability, thermophoresis, Brownian motion, or heat generation/absorption characteristic while it is decreased by improving the Prandtl number or the surface tension. Concentration levels are improved with higher permeability parameter or thermophoresis while they are decreased by higher Brownian motion, Schmidt number or surface tension (Figure 9). Density of motile microorganism is improved with higher magnetic parameter, thermophoresis, Brownian motion, or Schmidt number while it is decreased by higher Prandtl number, Lewis number, Peclet number, or surface tension. Close to the surface, the concentration levels are in-

creased by increasing the Prandtl number while the reverse happens apart from the surface. Close to the surface, the temperature profile is slightly increased by increasing the Schmidt number while the reverse takes place apart from the surface. Close to the surface, the concentration levels are slightly decreased by increasing the heat generation/absorption parameter while the reverse happens apart from the surface.

References

1. Arifin NM, Nazar R, Pop I (2010) Marangoni-driven boundary layer flow in nanofluids, in: Proc. 2010 Int. Conf. Theor. Appl. Mech. 2010 Int. Conf. Fluid Mech. Heat Mass Transf., World Scientific and Engineering Academy and Society (WSEAS), Stevens Point, Wisconsin, USA 2010: pp: 32-35.
2. Golia C, Viviani A (1986) Non isobaric boundary layers related to Marangoni flows, *Meccanica* 21: 200-204.
3. Chamkha AJ, Pop I, Takhar HS (2006) Marangoni Mixed Convection Boundary Layer Flow, *Meccanica* 41: 219-232.
4. Pop I, Postelnicu A, Groşan T (2001) Thermosolutal Marangoni Forced Convection Boundary Layers, *Meccanica* 36: 555-571.
5. Christopher DM, Wang B (2001) Prandtl number effects for Marangoni convection over a flat surface. *Int J Therm Sci* 40(6): 564-570.
6. Hamid RA, Arifin NM, Nazar R, Ali F (2011) Radiation effects on Marangoni convection over a flat surface with suction and injection. *Malaysian Journal of Mathematical Sciences* 5(1): 13-25.
7. Lin Y, Zheng L (2015) Marangoni boundary layer flow and heat transfer of copper-water nanofluid over a porous medium disk. *AIP Adv* 10(5).
8. Tiwari AK, Raza F, Akhtar J (2017) Mathematical model for Marangoni convection MHD flow of carbon nanotubes through a porous medium. *IAETSD J Adv Res App Sci* 4 (7): 216-222.
9. Raju KV, Prasad PD, Raju MC, Sivaraj R (2018) Numerical Investigation on MHD Marangoni Convective Flow of Nanofluid through a Porous Medium with Heat and Mass Transfer Characteristics. *Int J Eng Technol* 7(4): 256-260.
10. Pedley TJ, Kessler JO, Lighthill MJ (1987) The orientation of spheroidal microorganisms swimming in a flow field, *Proc R Soc Lond B Biol Sci* 231(1262): 47-70.
11. Pedley TJ, Hill NA, Kessler JO (1988) The growth of bioconvection patterns in a uniform suspension of gyrotactic micro-organisms. *J Fluid Mech* 195: 223-237.
12. Kessler, JO (1985) Hydrodynamic focusing of motile algal cells, *Nature* 313: 218-220.
13. Kessler JO (1985) Co-operative and concentrative phenomena of swimming micro-organisms. *Contemp Phys* 26(2): 147-166.
14. Hill NA, Pedley TJ, Kessler JO (1989) Growth of bioconvection patterns in a suspension of gyrotactic micro-organisms in a layer of finite depth. *J Fluid Mech* 208: 509-543.
15. Ghorai S, Hill NA (1999) Development and stability of gyrotactic plumes in bioconvection. *J Fluid Mech* 400: 1-31.
16. Ghorai S, Hill NA (2000) Wavelengths of gyrotactic plumes in bioconvection. *Bull Math Biol* 62(3): 429-450.
17. Ghorai S, Hill NA (2007) Gyrotactic bioconvection in three dimensions. *Phys of Fluids* 19(5): 054107.
18. Hillesdon AJ, Pedley TJ (1996) Bioconvection in suspensions of oxytactic bacteria: linear theory. *J Fluid Mech* 324: 223-259.
19. Hopkins MM, Fauci LJ (2002) A computational model of the collective fluid dynamics of motile micro-organisms. *J Fluid Mech* 455: 149-174.
20. Kuznetsov AV (2005) The onset of bioconvection in a suspension of gyrotactic microorganisms in a fluid layer of finite depth heated from below. *Int Commun Heat Mass Transf* 32(5): 574-582.
21. Zeng L, Pedley TJ (2018) Distribution of gyrotactic micro-organisms in complex three-dimensional flows. Part 1. Horizontal shear flow past a vertical circular cylinder. *J Fluid Mech* 852: 358-397.
22. Vajravelu K, Hadjinicolaou A (1993) Heat transfer in a viscous fluid over a stretching sheet with viscous dissipation and internal heat generation. *Int Commun Heat Mass Transf* 20(3): 417-430.



This work is licensed under Creative Commons Attribution 4.0 License

Your next submission with Juniper Publishers will reach you the below assets

- Quality Editorial service
- Swift Peer Review
- Reprints availability
- E-prints Service
- Manuscript Podcast for convenient understanding
- Global attainment for your research
- Manuscript accessibility in different formats

(Pdf, E-pub, Full Text, Audio)

- Unceasing customer service

Track the below URL for one-step submission

<https://juniperpublishers.com/online-submission.php>